International Journal of Mechanical, Industrial and Aerospace Sciences
ISSN: 2517-9950
Vol:3, No:10, 2009

A New Hybrid Method to Correct for Wind Tunnel Wall- and Support Interference On-line

B.J.C. Horsten and L.L.M. Veldhuis

Abstract—Because support interference corrections are not properly understood, engineers mostly rely on expensive dummy measurements or CFD calculations. This paper presents a method based on uncorrected wind tunnel measurements and fast calculation techniques (it is a hybrid method) to calculate wall interference, support interference and residual interference (when e.g. a support member closely approaches the wind tunnel walls) for any type of wind tunnel and support configuration. The method provides with a simple formula for the calculation of the interference gradient. This gradient is based on the uncorrected measurements and a successive calculation of the slopes of the interference-free aerodynamic coefficients. For the latter purpose a new vortex-lattice routine is developed that corrects the slopes for viscous effects. A test case of a measurement on a wing proves the value of this hybrid method as trends and orders of magnitudes of the interference are correctly determined.

Keywords—Hybrid method, support interference, wall interference, wind tunnel corrections.

I. Introduction

Besides wind tunnel wall interference corrections, support interference corrections are commonly applied to wind tunnel test results. Applying these corrections to the measurements increases the accuracy of the determination of free-flight characteristics of aircraft configurations. Determining support interference corrections has seemed more complex than determining wall interference corrections. This is because wall interference is seen as a far-field disturbance and can hence be determined accurately using inviscid calculation methods (AGARDograph 336 [1]). The problem of support interference is more complicated because it also involves viscous near-field effects with a very complex flow topology (Horsten [2]). Amongst the most common methods for determining support interference are: Dummy measurements (Eckert [3]), CFD calculations such as vortex-lattice calculations (Vaucheret [4]), Panel-Code calculations (Mokry [5]) and even Navier-Stokes calculations (Petterson [6]). Performing dummy measurements has always been an elaborate and sometimes expensive task. Generally speaking, the accuracy of dummy measurements is perceived as high, being twice the standard deviation of the balance system accuracy used to measure the forces and moments. The accuracy of CFD calculations usually does not reach that level. Including more physics in the simulation might increase the accuracy but also the computational effort. Another major disadvantage is the modeling effort. Changing angles of attack and sideslip sometimes necessitates re-modeling depending on the degrees of freedom of the support structure.

B.J.C. Horsten is a PhD. student at the Department of Aerodynamics at the Faculty of Aerospace Engineering, Delft University of Technology, Kluyverweg 2, 2629 HT, Delft, The Netherlands. Email: B.J.C.Horsten@tudelft.nl

L.L.M. Veldhuis is an associate professor at the Department of Aerodynamics at the Faculty of Aerospace Engineering, Delft University of Technology, Kluyverweg 2, 2629 HT, Delft, The Netherlands. Email: L.L.M.Veldhuis@tudelft.nl

Manuscript received May 27, 2009; revised September 7, 2009.

In the present work a new method is presented that determines wall interference, support interference and all the residual interference effects (consider the additional disturbance on the model when the support structure approaches the wind tunnel walls closely) for all types of wind tunnels and support configurations. The method is fast and satisfies accuracy requirements. It omits the task of performing dummy measurements and extensive modeling for CFD purposes. It combines uncorrected measurements with fast vortex-lattice calculations (it is a hybrid method) making it a suitable method for on-line use during a wind tunnel test. In order to increase the accuracy of this method, a vortex-lattice routine is developed correcting for the effects of viscosity in the calculation-part of the method without losing the advantage of short calculation times. The following sections will demonstrate the theoretic principle of this hybrid method. Based on accuracy requirements it will be explained that a vortex-lattice routine correcting for viscous effects is needed to maintain the advantages of both speed and accuracy. The structure of this newly developed vortex-lattice routine is explained. A test case showing the application of the method will be presented and the results will be discussed.

II. Theory

Assume a wind tunnel model being attached to a support configuration in a wind tunnel. The configuration of the model as the support configuration and the wind tunnel layout are of no importance at all. A measurement can be performed using this model at a certain angle of attack $\alpha = \alpha_1$ and angle of sideslip $\beta = \beta_1$. It can now be said that:

$$C_{i_1} = C_{i_{und_1}} + \Delta C_{i_{int_1}} \tag{1}$$

In Equation 1, the measured value of a certain parameter (it could be the lift-coefficient for example) consists of a “clean” true value (with the subscript “und” for “undisturbed”) and an interference part from the support structure, wind tunnel walls and the residual interference (with the subscript “int” for “interference”). Assume that the value of this interference term is known for this first measurement point. This measurement is then corrected for the interference according to:

$$C_{i_{und_1}} = C_{i_1} - \Delta C_{i_{int_1}} \tag{2}$$

The next measurement point is taken at α = α_2 and β = β_1 (here for convenience only angle of attack polars are considered. The theory is also applicable to angle of sideslip polars). At this new measurement point:

$$\begin{aligned} C_{i_2} &= C_{i_{und_2}} + \Delta C_{i_{int_2}} \longrightarrow \\ C_{i_2} &= C_{i_{und_1}} + \frac{\partial C_{i_{und_1}}}{\partial \alpha}(\alpha_2 - \alpha_1) + ... \\ & \quad \Delta C_{i_{int_1}} + \frac{\partial \Delta C_{i_{int_1}}}{\partial \alpha}(\alpha_2 - \alpha_1) \end{aligned} \tag{3}$$

When Equation 1 is subtracted from Equation 3, the result is as follows:

$$\begin{aligned} C_{i_2} - C_{i_1} &= \frac{\partial C_{i_{und_1}}}{\partial \alpha}(\alpha_2 - \alpha_1) + ... \\ & \quad \frac{\partial \Delta C_{i_{int_1}}}{\partial \alpha}(\alpha_2 - \alpha_1) \end{aligned} \tag{4}$$

The gradient of the interference can now be calculated as:

$$\frac{\partial \Delta C_{i_{int_1}}}{\partial \alpha} = \frac{(C_{i_2} - C_{i_1}) - \frac{\partial C_{i_{und_1}}}{\partial \alpha}(\alpha_2 - \alpha_1)}{(\alpha_2 - \alpha_1)} \tag{5}$$

The first part of the numerator in Equation 5 follows directly from the measurements. The second part of the numerator is found by calculations (here, the slope of the coefficient under consideration is calculated at angle of attack α = α_1 and angle of sideslip β = β_1). A very efficient way (in the light of time- and cost-reduction) of calculating this gradient is by the use of a vortex-lattice code. This method is able of calculating the necessary characteristics fast and for a variety of lifting surface configurations, angles of attack and angles of sideslip. When the gradient of the interference is calculated, this new measurement point can be corrected as follows:

$$\Delta C_{i_{int_2}} = \Delta C_{i_{int_1}} + \frac{\partial \Delta C_{i_{int_1}}}{\partial \alpha}(\alpha_2 - \alpha_1) \tag{6}$$

and the measurement can be corrected right away according to:

$$C_{i_{und_2}} = C_{i_2} - \Delta C_{i_{int_2}} \tag{7}$$

When this correction is performed, the next measurement point can be taken, and the procedure is repeated.

III. Advantages and Disadvantages of the Method

Some advantages of the method as described in the last section are:

1) No mathematical representation of the wind tunnel and support are necessary: The method is applicable for every test configuration
2) The method combines the best of both worlds: On one hand, accuracy is presumed high because measurements are taken (the accuracy bandwidth is proportional to twice the standard deviation of the balance accuracy). On the other hand a very fast numerical method is chosen such as to calculate the gradients of parameters of interest. The calculation is fast and reasonably accurate: Vortex-lattice codes are known to be able to calculate the right trends and gradients whereas the absolute value of the parameters can be off. These absolute values are however not of interest
3) Because of the flexibility of the vortex-lattice code, different configurations (tail on/tail off, including elevator/rudder/flap-deflections) can be calculated
4) The method works for angle of attack- and angle of sideslip-polars
5) Calculation and correction of the interference can be performed on-line

The most important disadvantages of this method are:

1) Because of the use of a vortex-lattice code, this method is applicable to within the restrictions as provided by these type of codes:
   - The method is applicable in the linear angle of attack- and angle of sideslip ranges
   - When the disturbance parameter of interest would be the drag-coefficient, the vortex-lattice calculation will only provide with the gradient of the induced drag. The profile drag is not included because no viscous effects are simulated by a vortex-lattice code

   This disadvantage can be relieved when a numerical method is used that is able to correct for the effects of viscosity. Such a method is developed and will be discussed in section V
2) As initial condition the first interference term has to be known. From this term on, the residual interference pattern is calculated. It is wise to choose the initial condition where the interference is small (e.g. at an angle of attack and angle of sideslip of 0 [deg]). If chosen at a point where the interference is not small, a substantial error might be introduced (caused by the inaccuracy of the determination of this interference) that is maintained in the entire (α, β)-domain of the determined corrections

When the advantages and disadvantages of this method are known, it is wise to look at the accuracy of the method because this accuracy will determine the success of the method in calculating the value of wind tunnel wall- and support interference. A discussion on the accuracy is given in the next section.

IV. Distinguishable Error Sources

When Equation 6 is considered, it becomes clear that the accuracy of the determination of the interference at a new measurement point depends on the following factors:

1) The accuracy of the determination of the interference of the previous point. When the first interference term with this method is calculated, the accuracy is determined by the accuracy of the initial condition. This implies that it

is of utmost importance to choose the initial condition in terms of α and β properly. It is therefore wise to choose the initial condition at the point where the total interference is expected to be minimal and accurately known. Usually this is at (α, β) = 0 [deg]. When large errors (measurement errors) are introduced here, these errors will be maintained throughout the whole polar

2) The determination of the interference gradient. According to Equation 5, the accuracy in the determination of this gradient is a result of:
   - The measurement accuracy (consider the first term in the numerator of Equation 5)
   - The accuracy with which the interference-free coefficient gradients are determined (by a vortex-lattice code for example)
3) It will be clear that the step size $\Delta\alpha$ or $\Delta\beta$ also affect the accuracy using this method because a linear approach is adopted. During wind tunnel measurements, this step size is usually rather large (O(0.5-1.0) [deg]). Therefore it is recommendable when using this method to first measure a polar, spline the results and interpolate the results to a fine grid (O(0.01 [deg])). The same is done for the results of the vortex-lattice calculations. This enables an analysis of the interference with a higher accuracy

On the whole it can be said that the most troublesome accuracy requirement is on the determination of the interference-free gradients by a vortex-lattice code. When it is assumed that the initial condition of a calculation has an error of 0 ("an exact determination of the interference"), the errors in the calculation of the interference for the upcoming measurement points are given by:

$$\begin{aligned}
Calculation\,1 \rightarrow & E\left(\Delta C_{i_{int_1}}\right) = 0 \\
Calculation\,2 \rightarrow & E\left(\Delta C_{i_{int_2}}\right) \propto E\left(\Delta C_{i_{int_1}}\right) + ... \\
& E\left(\frac{\partial C_{i_{und_1}}}{\partial \alpha}\left(\alpha_2 - \alpha_1\right)\right) \\
Calculation\,3 \rightarrow & E\left(\Delta C_{i_{int_3}}\right) \propto E\left(\Delta C_{i_{int_2}}\right) + ... \\
& E\left(\frac{\partial C_{i_{und_2}}}{\partial \alpha}\left(\alpha_3 - \alpha_2\right)\right) = ... \\
& E\left(\frac{\partial C_{i_{und_1}}}{\partial \alpha}\left(\alpha_2 - \alpha_1\right)\right) + ... \\
& E\left(\frac{\partial C_{i_{und_2}}}{\partial \alpha}\left(\alpha_3 - \alpha_2\right)\right) \\
& ...
\end{aligned} \tag{8}$$

Equation set 8 is only valid when it is assumed that the error made in the determination of the first term in the numerator of Equation 5 is small (e.g. the actual measurements have a high accuracy). The equations show that the error in the method is decreased when:

1) The interference-free gradients of the coefficients are properly calculated
2) The step-size in the analysis is small

It can be seen in Equation set 8 that when the vortex-lattice code systematically over- or under-predicts the value of the interference-free coefficient gradients, the error will grow during the calculation of the interference in a polar. When however the true values are scattered around the prediction by the vortex-lattice code (some values are under-estimated and other values are over-estimated) it is seen that the errors have the tendency of canceling each other out.

It is of importance that the calculated values of the interference-free gradients by the vortex-lattice code closely approximate the true values. To increase the accuracy of this method and the operational boundaries, correcting for the effects of viscosity is unavoidable. For this purpose, a new vortex-lattice routine is developed. This routine is discussed in the next section.

V. Development of a New Vortex-Lattice Routine Correcting for the Effects of Viscosity

Successively modeling the viscous gradients of the aerodynamic coefficients of a configuration in the wind tunnel is the key to the development of a new vortex-lattice routine implementable in the hybrid method as discussed in this paper. The new vortex-lattice routine combines 3D steady vortex-lattice calculations using the program "Athena Vortex-Lattice" (AVL) with a 2D viscous airfoil calculation in "XFOIL". Various calculations with these methods are necessary to arrive at the values of the polar-gradients of interest.

The vortex-lattice routine starts by defining the lifting surfaces of interest by means of user input. At current, the first version of this program is designed to deal with the main wing only. The main wing is defined by identifying its typical sections in 3D space. The sections are defined by describing the mean camberline (by customized coordinates describing the mean camberline or the 4-digit designation of the 4-digit NACA series). Wing sections are designated a chord. Between these wing sections, linear interpolation is applied on the camberline and chord length thereby defining the wing surface. Geometric features such as taper, sweep and dihedral are included by a proper definition of the section placements. Twist can also be included by defining a local angle of attack (between the sections, the local twist value is linearly interpolated). The presence and deflection angle of flaps can also be defined. Besides geometrical information describing the wing surface, parameters describing the freestream (Mach number, angle of attack and angle of sideslip for instance) are also prescribed. All the data is written to an input file for the program AVL.

The input file is read by AVL and the geometrical description of the wing is translated to a numerical discretization by the

placement of a number of horseshoe vortices on the wing surface to model the circulation. The wing is represented by a number of spanwise bound-vortex collections placed at various chordwise stations and ending in free trailing vortices extending downstream in analogy with Helmholtz's vortex theorem. Based on the boundary conditions described by the freestream parameters and the flow tangency condition (prescribed by the law of Biot-Savart) at the collocation points on the surface of the wing, the strength of the horseshoe vortices is calculated leading to the calculation of the inviscid lifting properties of the wing at given freestream conditions. Fig. 1 shows an example of a typical wing that is implemented by AVL. The wing consists of 4 sections with a NACA 2315 profile. Features such as taper, sweep and dihedral are included. Information about the wing properties is given in Table I. At the inboard part of the wing a flap is specified from 80% of the local chord to the trailing edge. Fig. 1 clearly shows the trailing legs of the horseshoe vortices discretizing the wing.

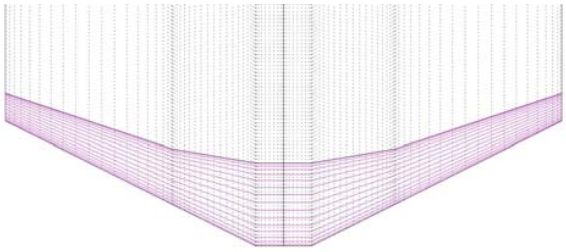

Fig. 1. An example of a wing as implemented by AVL

TABLE I
WING PROPERTIES AS IMPLEMENTED BY AVL

Parameter	Value
Taper inner wing	0.67
Leading edge sweep inner wing	26.6 [deg]
Dihedral inner wing	1.9 [deg]
Taper outer wing	0.50
Leading edge sweep outer wing	26.6 [deg]
Dihedral outer wing	1.9 [deg]
Profile	$NACA-2315$
Reynolds Number	2.5x10^6

At certain freestream conditions AVL is capable of calculating the inviscid aerodynamic characteristics of the prescribed wing. Of particular interest is the spanwise distribution of induced angle of attack. This value can be visualized by a Trefftz-plane plot as given by Fig. 2.

The spanwise distribution of the induced angle of attack is used in order to calculate the effective angle of attack of the sections describing the wing as follows:

$$\alpha_{eff} = \alpha_\infty - \alpha_{ind} + \alpha_{wash} \tag{9}$$

In Equation 9, the effective angle of attack is calculated by

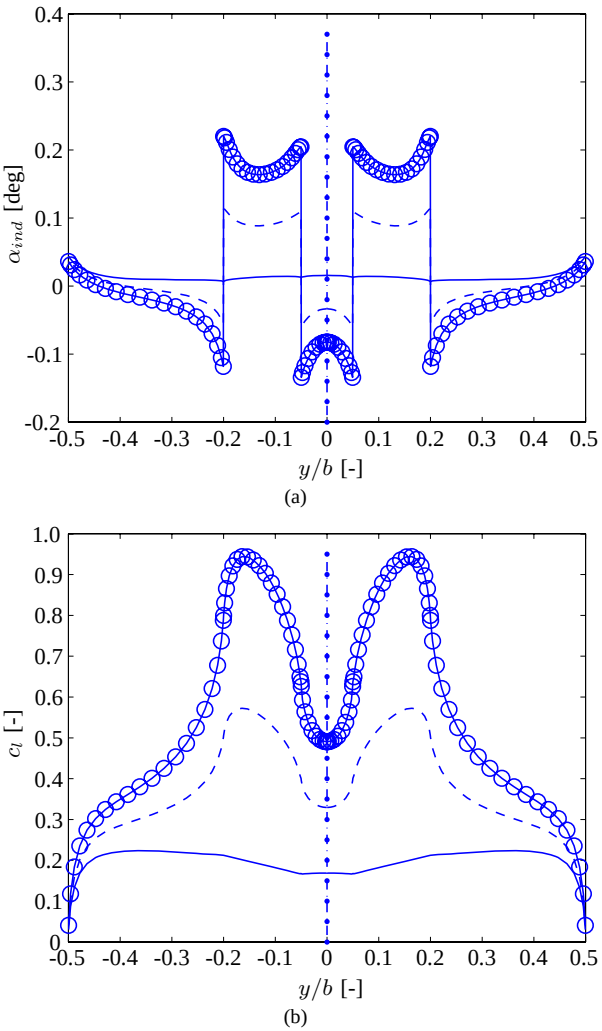

Fig. 2. A Trefftz-plane plot of the spanwise distribution of (a) Induced angle of attack α_{ind} (b) Local lift-coefficient c_l for the discretized wing at α_∞ = 0°, β_∞ = 0° and V_∞ = 60 [m/s] with various flap settings: — = 0°, - - - = 10° and -o- = 20°. In the figure, the symmetry line of the configuration is also indicated

performing linear operations on the freestream angle of attack α_∞, the induced angle of attack α_{ind} and on the local washout of the section α_{wash}. Consider the case for a particular value of α_∞. For this freestream angle of attack the spanwise distribution of effective angle of attack is calculated. For every section, 2D XFOIL calculations are performed, both inviscid and viscous (at the local Reynolds number). The calculations are performed for a wide range of angles of attack spanning a complete angle of attack polar. This leads to viscous and inviscid polars for every section. The calculated value of the effective angle of attack of every section is then used to find the inviscid and viscous 2D lift-coefficient for every section spanning the wing by piecewise cubic Hermite interpolation. Define the difference between 2D inviscid and viscous lift of a particular wing section at α_{eff} as dC_l. This difference dC_l is caused by the effects of viscosity. It can be translated to a shift in local angle of attack from the inviscid polar to the

viscous polar as follows:

$$d\alpha_{section} = \frac{dC_l}{\frac{\partial C_l}{\partial \alpha}_{inv}} \tag{10}$$

In Equation 10 it is seen that the inviscid lift-slope is used in order to calculate the shift in angle of attack that is necessary to correct the 2D inviscid lift for the effects of viscosity. The inviscid lift-slope is used here because the viscous lift-slope will reach values of zero at higher angles of attack (near the profile stall condition) thereby introducing singularities in Equation 10. The implication of the above is now the following. If at a certain angle of attack α_∞ the induced angles of attack are calculated by an inviscid calculation (in AVL), the XFOIL results will enable the calculation of a correction in angle of attack for all the sections to transform the 2D inviscid lift-coefficient to 2D viscous lift-coefficients of the sections. This shift in local angle of attack can be super-imposed on the local section twist of the airfoil. This enables a new AVL calculation with a "morphed" wing. The output of this calculation will provide with a lift distribution that is corrected for the local effects of viscosity.

It will be clear that for every angle of attack α_∞ the local twist correction on every section is necessary (because changing the freestream angle of attack changes the spanwise distribution of α_{ind}). This also means that in order to calculate a lift polar that is corrected for viscous effects (consisting of multiple angles of attack), new *N* corrected AVL calculations are ran implementing *N* new twist distributions over the wing. Fig. 3 gives the twist correction $\Delta\alpha_{tw}$ at various angles of attack for the sections spanning the wing. Implementing the new twist shown in Fig. 3 leads to the calculation of a new lift distribution over the wing as shown in Fig. 4 where the inviscid and "viscous" lift distributions in the Trefftz plane are given. Fig. 5 provides with a comparison of the calculated inviscid vs. corrected lift polars.

Comparing Fig. 3, 4 and 5 it is seen that for some sections defining the wing the twist correction is significant. This twist correction leads to a new lift distribution as calculated by AVL. Integrating this lift distribution of the wing at a given value of α_∞ provides with the value of the corrected lift-coefficient. When comparing the "viscous" and inviscid lift curves it is seen that the viscous curve indeed shows non-linear behavior at high angles of attack indicating stall behavior.

With the new corrected spanwise lift distribution as calculated by AVL, a corrected induced drag distribution is also calculated. The complete drag of the wing is however calculated by adding the integrated value of the induced drag to the integrated value of the parasite drag. The calculation of the spanwise distribution of the parasite drag is performed as follows: Using the corrected calculation of the induced angles of attack, the effective angle of attack α_{eff} of the sections spanning the wing are re-calculated. Using the two-dimensional XFOIL results, the value of the profile drag

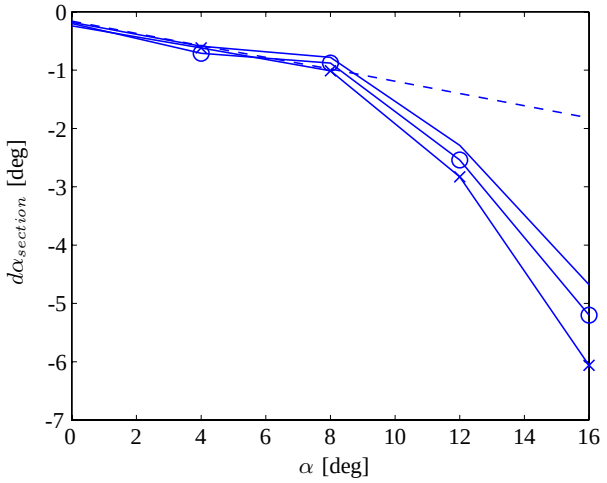

Fig. 3. Angle of attack dependency of the twist corrections of various wing stations (expressed in the value of y/b): — = 0, - - - = ±0.05, -o- = ±0.20 and -x- = ±0.50

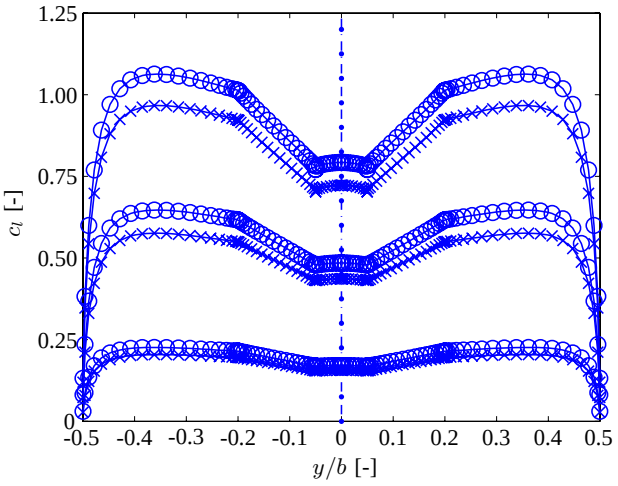

Fig. 4. Trefftz plane plot of the inviscid (-o-) and "viscous" (-x-) (or, corrected for the effects of viscosity) lift distributions over the wing at various angles of attack. From bottom to top the results for α = 0°, 4° and 8° are found. In the figure, the symmetry line of the configuration is also indicated

can be found for the sections by interpolation using this value of the effective angle of attack. The spanwise positions on the wing in between the sections are then evaluated by linear interpolation of the profile drag of the sections. Once the spanwise distributions of induced drag and parasite drag are calculated, the complete drag of the configuration follows by integration of the drag over the wing. An example of a resulting drag polar compared to the uncorrected inviscid result is given in Fig. 6.

In this section, an example of the new vortex-lattice routine is demonstrated. By coupling the programs XFOIL and AVL, corrections for the absence of viscosity in the AVL calculations can be calculated for the lift polar and drag polar of a wing.

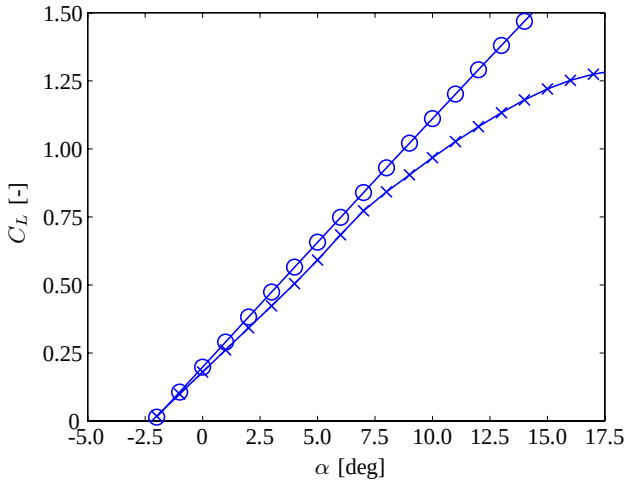

Fig. 5. Inviscid (o) and "viscous" (x) lift polars of the wing

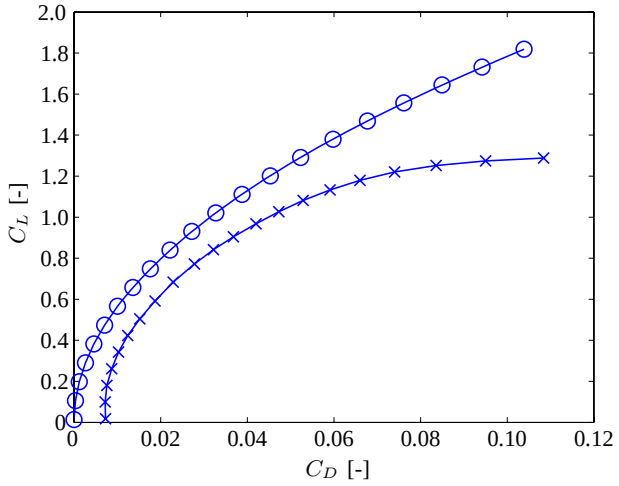

Fig. 6. Inviscid (-o-) and "viscous" (-x-) drag polars of the wing

It is recognized that this method might not demonstrate the correct absolute values of the resulting polars when compared to for instance measurements. However these values are not of importance. This method is setup in order to include the effects of viscosity in the aerodynamic derivatives. For this purpose, the new vortex-lattice method seems to work good enough. This is demonstrated in the following section by a test case.

VI. A Demonstration of the Hybrid Method Using the New Vortex-Lattice Routine

As an example to demonstrate the validity of the hybrid method to correct for wall- and support interference, a test case is setup. This test case concerns the measurement of a finite wing in any wind tunnel. In the wind tunnel, this wing is disturbed by the presence of wind tunnel walls and model support members. Corrected aerodynamic polars of such a measurement are available to the author and will from now on be regarded as "unaffected". The characteristics of the test case wing are given in Table II.

TABLE II
Wing properties of the hybrid method test case

Parameter	Value
Wing Span	1.28 [m]
Mean Aerodynamic Chord	0.24 [m]
Wing Taper Ratio	1.00
Wing Sweep	0.0 [deg]
Wing Dihedral	0.0 [deg]
Profile	$NACA-64_2\,(A)\,015$
Reynolds Number	1.0x10^6

In order to demonstrate the wide applicability of the hybrid method, the measured unaffected data is contaminated by a random error simulating wall- and support interference for any wind tunnel using any support structure for the wing. In this test case a random error for both the unaffected value of lift- and drag-coefficients is generated by a random number generator. This random error is added to the clean measurements to generate "uncorrected data". The hybrid method will be used on this uncorrected data in order to back-calculate the value of the interference on both lift- and drag-coefficients.

In using the hybrid method, an approximation of the slopes of the interference-free aerodynamic characteristics of interest (C_L and C_D) is calculated by the new vortex-lattice routine. The results of this exercise are given in Fig. 7. In the figure, the calculated characteristics for a regular inviscid implementation in AVL are also given.

It is seen in Fig. 7(a) that applying the new vortex-lattice routine greatly improves the determination of the lift-slope compared to the inviscid result. Fig. 7(b) shows not much difference, an indication that for the considered angles of attack the drag-slope is not much affected by viscosity. These characteristics are used in order to back-calculate the values of the interference using the uncorrected data according to Equations 5 and 6. The result of this exercise is given in Fig. 8.

It is seen in Fig. 8(a) that the interference as generated by the random number generator is reproduced fairly accurate by applying the new vortex-lattice routine in the hybrid method. Both trend and order of magnitude are predicted properly. It is seen that for increasing angle of attack the error of the method increases. This is due to the fact that from α = 8 [deg] onwards a systematic underprediction of the lift-slope is calculated as seen in Fig. 7(a). According to Equation set 8, this leads to an accumulation of the error. Possible error divergence is a great disadvantage of this method. Applying a regular inviscid vortex-lattice code to calculate the slope of the lift-coefficient results in erroneous results. Because the slope of the drag-coefficient versus angle of attack for both numerical methods show a fair agreement (as pointed out earlier), the back-calculated value of the drag-interference also shows an agreement with the pre-generated pattern. Applying the new vortex-lattice routine however results in a more accurately calculated interference pattern when

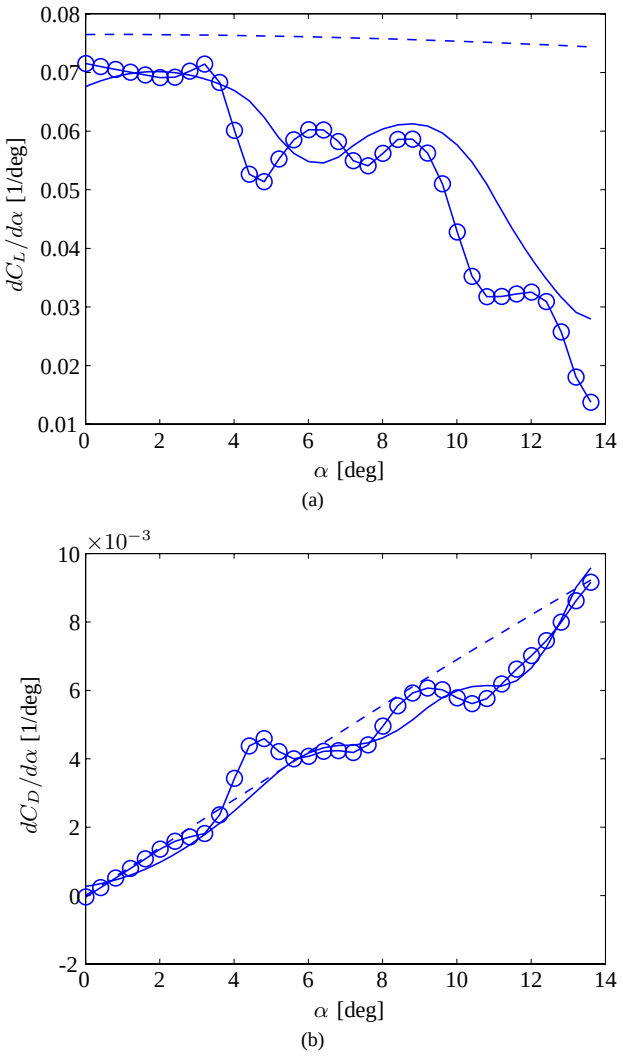

Fig. 7. Measured and calculated values of the slopes of (a) The lift-coefficient (b) The drag-coefficient. — = Measured values, - - - = inviscid vortex-lattice results and -o- = results of the new vortex-lattice routine correcting for the effects of viscosity

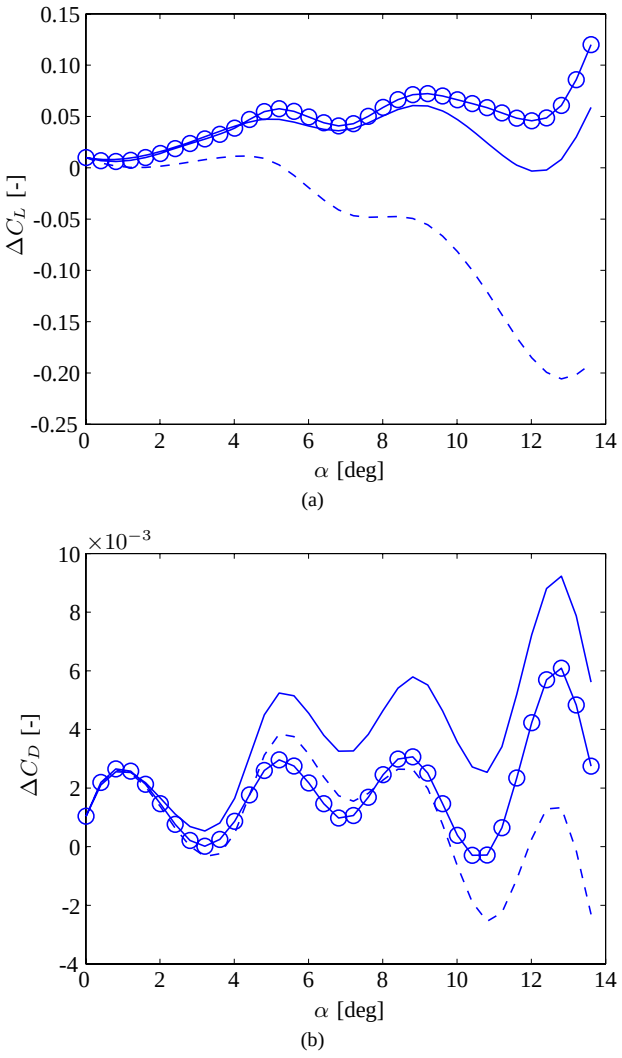

Fig. 8. "Measured" and calculated values of the interference on (a) The lift-coefficient (b) The drag-coefficient. — = Created by the random number generator, - - - = calculated using an inviscid vortex-lattice calculation and -o- = calculated using the new vortex-lattice routine correcting for the effects of viscosity

compared to the analytical results from the random number generator. Applying the calculated values of the interference to the uncorrected lift- and drag-coefficients leads to the final corrected data. These can be compared to the values of uncorrected and "true" (data uncontaminated by the random number generator) results. These results are given in Fig. 9.

It is clear from Fig. 9 that the hybrid method is able of calculating the values of the unaffected lift- and drag-coefficients quite reasonably. It is clearly seen that applying a vortex-lattice routine correcting for viscous effects is preferable above the inviscid variant. Although this method is not yet able to calculate the values of the interference to within typical wind tunnel balance accuracy (as can be done using e.g. dummy measurements), it is cheap, fast and gives a satisfying indication of the trends and orders of magnitude of the interference.

VII. Conclusion

This paper has presented a hybrid method (based on both uncorrected wind tunnel measurements and calculations) of correcting for wind tunnel wall- and support interference on-line during a wind tunnel test. Unlike tiresome and expensive dummy measurements and CFD calculations, this method has the advantage of being cheap, fast and containing a satisfying accuracy. It is applicable for every type of wind tunnel and support structure and resolves the complete interference package (consisting of wall- and support interference and also the residual interference terms). The method provides with a simple formula for the calculation of the interference gradient. This gradient is based on the uncorrected measurements and a successive calculation of the slopes of the interference-free aerodynamic coefficients. For this purpose a new vortex-lattice routine is developed that corrects these slopes for viscous

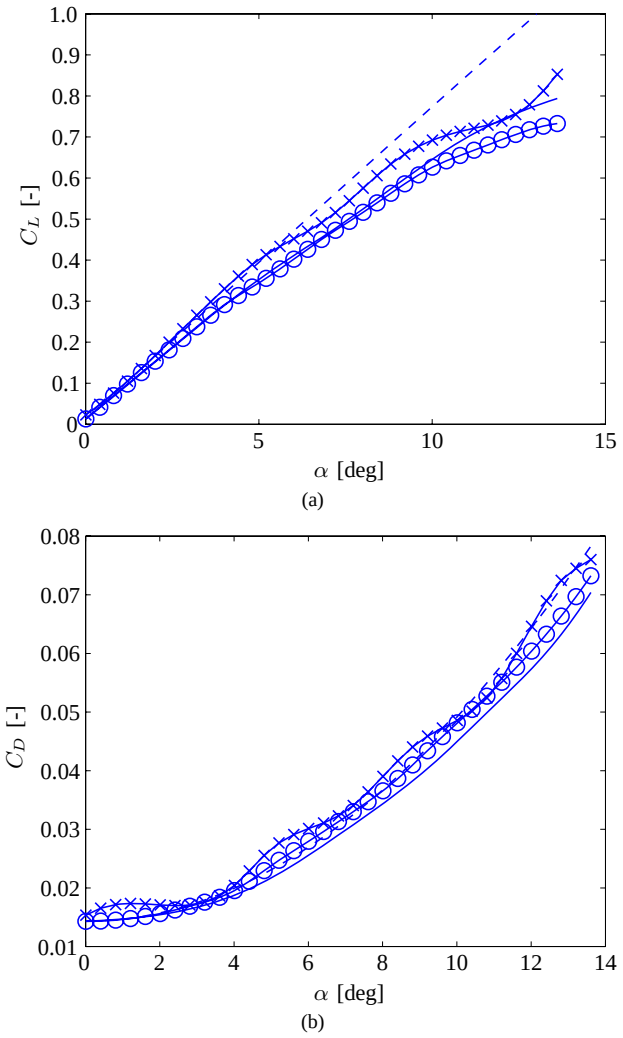

Fig. 9. Uncorrected, corrected (using the hybrid method) and "true" values of (a) The lift-coefficient (b) The drag-coefficient. — = True measured value, - - - = corrected using the hybrid method including an inviscid vortex-lattice calculation, -o- = corrected using the hybrid method including the new vortex-lattice routine correcting for the effects of viscosity and x = uncorrected

effects. This routine is a coupling shell between the 2D viscous "XFOIL" and the 3D inviscid vortex-lattice program "AVL". A test case of a measurement on a wing where the wing is affected by a randomly determined interference pattern proves the value of this hybrid method. Trends and order of magnitude of the corrections are predicted correctly. It is seen that the newly developed vortex-lattice calculation outperforms a regular vortex-lattice calculation in the hybrid method.

References

[1] B.F.R. Ewald, *AGARDograph 336: Wind Tunnel Wall Correction*. Canada Communication Group Inc., 1998.

[2] B.J.C. Horsten and L.L.M. Veldhuis, *Experimental and Numerical Results on Cavity Effects in Juncture Flow*. Conference Proceeding of the 38th Fluid Dynamics Conference and Exhibit, Seattle, Washington, United States, 2008.

[3] D. Eckert, *Correction of Support Influence on Measurements with Sting Mounted Wind Tunnel Models*. AGARD FDP Conference, Brussels, Belgium, 1993.

[4] X. Vaucheret, *Vortex Lattice Code For Computation of Any Wind Tunnel and Support Effects on Models*. La Recherche Aerospatiale, vol. 1(2), pp. 39-51, 1991.

[5] M. Mokry, *Evaluation of Combined Wall- and Support-Interference on Wind Tunnel Models*. AGARD-CP-535, 1994.

[6] K. Pettersson and A. Rizzi, *Aerodynamic scaling to free flight conditions: Past and present*. Progress in Aerospace Sciences vol. 44(4), pp. 295-313, 2008.

Bart J.C. Horsten B.J.C. Horsten (Bart) is a PhD. student at Delft University of Technology, Faculty of Aerospace Engineering, Aerodynamics Division. From 1999 to 2005 he was a college student at this faculty where he graduated in 2005 at the chair of Aerodynamics. During his graduation, he wrote a DNS code in order to perform laminar and turbulent simulations on riblet geometries. Aim of the research was to investigate the turbulent viscous drag reduction mechanisms caused by different riblet geometries implemented by the Immersed Boundary Method. After graduating at Delft University of Technology, a PhD. project was started in cooperation with DNW (German-Dutch Wind Tunnels) on the design of an Expert System for dealing with wind tunnel wall- and support interference. This is still his topic of research today.